"© 2015 IEEE. Personal use of this material is permitted. Permission from IEEE must be obtained for all other uses, in any current or future media, including reprinting/republishing this material for advertising or promotional purposes, creating new collective works, for resale or redistribution to servers or lists, or reuse of any copyrighted component of this work in other works."

G. Silva, F. Carpignano, F. Guerinoni, S. Costantini, M. De Fazio, S. Merlo, **Optical detection of the electro-mechanical response of MEMS micromirrors designed for scanning picoprojectors**, *IEEE Journal of Selected Topics in Quantum Electronics* (Special Issue on Optical Micro- and Nano-systems, 2015) Vol. 21, No. 4, pp. 2800110_1 – 2800110_10, Piscataway, NJ, USA (2015). DOI: 10.1109/JSTQE.2014.2369499

This is the author's version of an article that has been published in this journal. Changes were made to this version by the publisher prior to publication.
The final version of record is available at http://dx.doi.org/10.1109/JSTQE.2014.2369499

Optical Detection of the Electro-Mechanical Response of MEMS Micromirrors Designed for Scanning Picoprojectors

Gloria Silva, Francesca Carpignano, *Student Member, IEEE,* Federica Guerinoni, Sonia Costantini, Marco De Fazio and Sabina Merlo, *Senior Member, IEEE*

***Abstract*—Single-axis, rotational micromirrors actuated by comb finger structures have been designed, in view of their application in reflective scanning picoprojectors for laser beam displacement along two perpendicular directions to obtain a raster scan scheme. A resonant mirror operating at a frequency around 25 kHz, suitable for horizontal scans, as well as a linear mirror, suitable for vertical scan at the typical video refresh rate (60 Hz), have been fabricated by Silicon-on-Insulator technology and are illustrated in this work. We have in particular exploited the potentialities of semiconductor laser self-mixing interferometry, a powerful technique for characterizing the dynamic response of MEMS, for detecting the electro-mechanical response of both kinds of micromirrors. We report the results of the spot optical measurements performed on resonant and linear mirrors aimed at detecting the frequency of the fundamental rotational mode as well as of the in-plane and out-of-plane modes, close in frequency to the fundamental mode. We have experimentally demonstrated that the fabricated devices are suitable for high resolution miniaturized projectors, in terms of frequency response and scanning angle.**

***Index Terms*—Semiconductor Laser, Displays, Frequency Response, Microelectromechanical Systems, Micromirror, Optical Interferometry.**

I. INTRODUCTION

A growing field of applications for Micro-Electro-Mechanical-System (MEMS) devices is represented by reflective projection displays [1]-[4]. Reflective miniaturized laser projectors, often called picoprojectors, are expected to become more and more widespread, as a consequence of the increasing interest on exchanging and sharing directly from mobile devices (cell phones, tablets or digital cameras) multimedia contents, such as images, videos or presentations. The small screen size limitation of hand-held devices could be overcome by embedded picoprojectors allowing multimedia projection on various kinds of surfaces. Different picoprojector architectures have been proposed and developed. Two basic approaches can be identified, depending on the principle of image generation: the "micro display" and the "scanning projector." In the micro display approach, all pixels of a single image frame are generated at the same time. The major advantage is represented by the separation between the pixel generation and the projection steps, thus simplifying substantially the design procedure, even though the core device is quite complex, since it is a two-dimensional matrix containing all the required pixels for the desired resolutions. However, the refresh rate of all pixels is quite low since it is equal to the employed frame refresh rate and incoherent light sources can be used for the lighting system, leading to an extreme compactness of the whole device. A current picoprojector technology of this type is the Digital Light Processing (DLP) developed by Texas Instruments, based on a matrix (Digital Display Engine or DDE) of individual light switches (Digital Micromirror Devices or DMDs), one for each pixel, employing electrostatically controlled MEMS mirror structures for light digital modulation by changing the reflection direction into or out of the projection optics [5]-[10]. On the other hand, in scanning projectors, only one pixel at a time is generated. Hence, light is dynamically modulated while it is scanned through a path that covers the entire image frame, in a similar way as Cathode Ray Tube (CRT) devices work. The resulting image is thus reconstructed on the projecting surface by exploiting the light persistence on the retina. The tasks of image generation and projection cannot be separated anymore and have to be carefully co-designed. The main issues of this approach are the pixel generation rate that becomes very high, equal to the frame rate multiplied by the resolution, and the scanning mechanism, that requires a coherent light source and rotating mirrors for the horizontal and vertical scan directions. Despite of these issues, this type of device has the outstanding ability to create images always in focus on any surface at any distance, with the only constraint of the power density, which needs to be limited in accordance to laser safety requirements. Moreover, since scanning is continuous, the separation between each pixel appears smooth, leading to a perception of even higher image resolution. Picoprojectors belonging to this category are currently under development by different

Manuscript received September 30, 2014, revised November 4, 2014.
This work was partially supported by STMicroelectronics, Agrate Brianza, Mi, Italy.
G. Silva, F. Carpignano and S. Merlo are with Dipartimento di Ingegneria Industriale e dell'Informazione, Università degli Studi di Pavia, 27100 Pavia, Italy (Sabina Merlo, corresponding author, phone: +39-0382-985202; fax: +39-0382-422583; e-mail: merlo@ieee.org). M. De Fazio is with STMicroelectronics, Burlington, MA, USA. S. Costantini is with STMicroelectronics, Agrate Brianza (Mi), Italy. F. Guerinoni is with STMicroelectronics, Cornaredo (Mi), Italy.

Copyright (c) 2014 IEEE. Personal use is permitted. For any other purposes, permission must be obtained from the IEEE by emailing pubs-permissions@ieee.org.

This is the author's version of an article that has been published in this journal. Changes were made to this version by the publisher prior to publication.
The final version of record is available at http://dx.doi.org/10.1109/JSTQE.2014.2369499

companies, such as Bosch, Microvision, BTendo and STMicroelectronics. Development of biaxial micromirror devices started in the 1980s when Petersen presented the first electrostatically driven micromirror [11]. Those early devices were actuated through planar capacitors, which required huge electrodes underneath the mirror. Next, resonantly operating micromirrors actuated by electrostatic comb drives, with all electrodes in one layer, were presented [12]. Subsequently, a 1D scanning mirror device able to tilt quasi-statically around one axis was reported; the actuator was based on an electrostatic comb structure which consisted of two layers [13]. On these basis, Microvision Inc. developed its Integrated Photonics Module (IPM) scan engine [14], incorporating a biaxial MEMS scanner, that is a round mirror hinged through a linear torsional spring to a rigid frame. This frame is hinged to an outer fixed frame through another torsional spring that is placed along an orthogonal axis with respect to the first one. By exploiting magnetic actuation, the mirror can be rotated along two orthogonal axes and scan the incident light beam into a cone [15].

The alternative solution proposed by STMicroelectronics (STM) is based on an innovative “scanning laser projection engine” technology combined to the company expertise on MEMS, video processing and semiconductor technology [16]. This solution falls into the scanning projector approach, and it is similar to the one proposed by Microvision. Indeed, a single pixel is generated at a time by the combination of three RGB lasers. The solution proposed by STM employs two single-axis micromirrors: the first one is actuated at resonance and performs the horizontal scan, while the second one is driven by a 60 Hz saw tooth signal to perform the vertical scan. This particular solution has the advantage to completely separate the design of the fast resonant mirror from the slow linear one, thus allowing fine optimization of the design of each one of them. In order to project the image, the light beam formed by the superposition of three RGB laser beams is deflected horizontally at high frequency and then vertically scanned at the desired refresh rate, typically 60 Hz. For the resonant mirror, the resonance frequency of the fundamental torsional mode has to be in the order of 25 kHz and the scanning angle has to be at least 48°. For the linear mirror, the resonance frequency of the fundamental torsional mode has to be higher than 600 Hz and the scanning angle has to be at least 36° [17]-[21]. These parameters as well as spot size are known to affect display resolution. A product of tilt angle and mirror diameter of 12° x mm is considered the requirement for 1024 x 768 pixels resolution XGA displays [17], [18]. For both mirrors the drive voltage has to be lower than 250 V for proper integration in the final device. The driving circuitry for the final picoprojector is designed and realized by STM in HCMOS technology, which is limited to 250V.

Precise rotation of the mirrors is mandatory to provide accurate reconstruction of the image onto the projecting surface: the occurrence of spurious oscillating modes can create distortions in the image. In this paper, the resonant and the linear micromirrors designed and fabricated by STM are reported. In Sect. II, we briefly describe the principle of operation and the main fabrication steps for both models. Then, the performances of the fabricated mirrors are illustrated in terms of beam deflection angle and resonance frequency of higher order vibrating modes. In Sect. III, the optical noncontact methods applied for the characterization of the bare as-fabricated micromirrors are briefly explained. We have exploited in particular the potentialities of semiconductor laser feedback interferometry, a powerful technique for characterizing the dynamic response of microdevices, for detecting the electro-mechanical response of both kinds of micromirrors. In Sect. IV. and V. the results of the characterization of the resonant as well as of the linear mirror are then exposed.

II. Micromirror Design and Fabrication

The resonant micromirror for horizontal scan at approximately 25 kHz and the linear micromirror for operation at the video refresh rate of 60 Hz for vertical scans were designed and fabricated by STM using SOI (Silicon-On-Insulator) technology. Scanning Electron Microscope (SEM) images of the two kinds of micromirror are illustrated in Fig. 1. The circular resonant mirror (RM) has a 1-mm diameter, since the incidence of the incoming laser beam is always located at the same spot, while the linear mirror (LM) has a more elongated, rectangular shape, in order to collect the deflected beam from the first mirror for any position of the horizontal scan. The mirror diameter is chosen in order to guarantee the projected spot quality (the pixel of the image), without incurring in diffraction patterns [18].

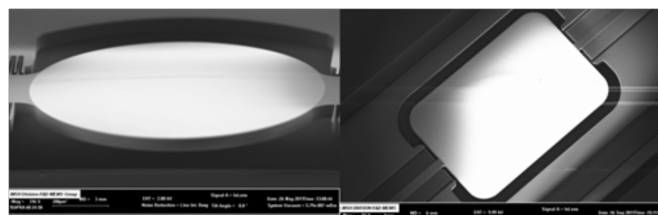

Fig. 1. SEM images of the resonant mirror (left) and of the linear mirror (right).

The RM device is 2.965 mm x 4.365 mm and 675-µm-thick; the LM chip is 2.250 mm x 7.750 mm and 725-µm-thick. These dimensions allow an assembled optical projection module that is less than 5-mm-thick, thus suitable for integration into currently available mobile phones. Both devices consist of a bulk silicon (Si) chip incorporating a rotating structure with the optical mirror suspended over a cavity via two silicon springs. Both MEMS micromirrors were designed to work at atmospheric pressure, thus no vacuum packaging is required.

Dynamic behavior of the electromechanical micromirrors was simulated by means of Finite Element Modeling (FEM) in order to predict the resonance modes in the design phase. STM MEMS design team, by means of proprietary tools commonly used by the Company to design the currently fabricated MEMS, performed numerical simulations; all design parameters were fine tuned to STM production processes and

Copyright (c) 2014 IEEE. Personal use is permitted. For any other purposes, permission must be obtained from the IEEE by emailing pubs-permissions@ieee.org.

This is the author's version of an article that has been published in this journal. Changes were made to this version by the publisher prior to publication.
The final version of record is available at http://dx.doi.org/10.1109/JSTQE.2014.2369499

their variation.

The micromirrors are electrostatically actuated by means of comb-finger structures, placed on stator and rotor. By applying an electrostatic voltage between the rotor and the stator, the fixed comb structure attracts the moving fingers, generating a mechanical torque, which induces the mirror rotation. The tilt angle is proportional to the square of the applied DC voltage.

The resonant micromirror is a planar device, as shown in Fig. 2: the stator and the rotor lay in the same plane, thus resulting in a simple structure, easy to fabricate [22]. Being on the same plane at rest, the comb fingers do not produce torque when a DC voltage is applied, but an AC signal needs to be applied at frequencies near the fundamental mode resonance, to induce rotation along its torsional axis.

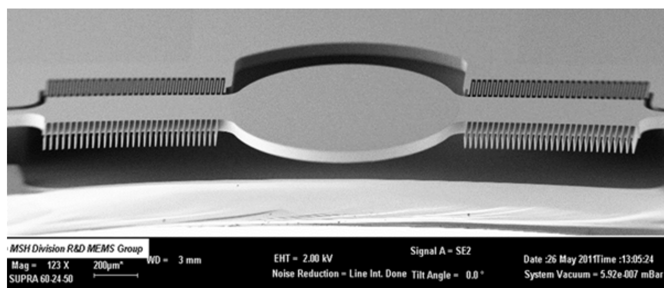

Fig. 2. SEM view of the resonant micromirror planar structure.

A sketch summarizing the fabrication steps of the resonant mirror is shown in Fig. 3. The MEMS structure is built starting from a silicon wafer (the starting wafer is the bulk structure of the device) in which cavities (to allow the suspended rotor to tilt) are realized by DRIE (Deep Reactive Ion Etching) (Step 1). The wafer is then oxidized and anodic bonded to a second wafer forming a SOI structure in which cavities are already present (Step 2). The top wafer is then thinned down to the desired thickness of 50 μm by means of Chemical Mechanical Polishing (CMP). A metal layer consisting of an Aluminum (Al) alloy is evaporated and patterned to form the mirror surface on the rotor and the electrical contact pads (Step 3). Since the RM device has only two electrical domains, the stator and the rotor, a trench etched on the top of the silicon layer down to the oxide underneath electrically separates the rotor and stator. The last process steps consist in the final release (by Reactive Ion Etching, RIE) of the rotor and comb fingers structures (suspended by two mechanical torsional springs), followed by a final oxidation to protect the surfaces (Step 4).

The process is simple, but faces several challenges: the mirror must be extremely planar (the maximum allowed curvature radius is 2 m, which means that the mirror should not deflect from the wafer plane by more than 0.5 μm). The reflective layer is made by an aluminum alloy specifically formulated to prevent hillock formation and oxidation, and to reduce the stress induced on the rotor structure while remaining highly reflective across the whole visible spectrum. On the other hand, the springs have to be designed to withstand inertial impact while assuring the desired torsional resonance frequency, and shifting the undesired vibration modes to frequencies that will not be excited by the driving signal.

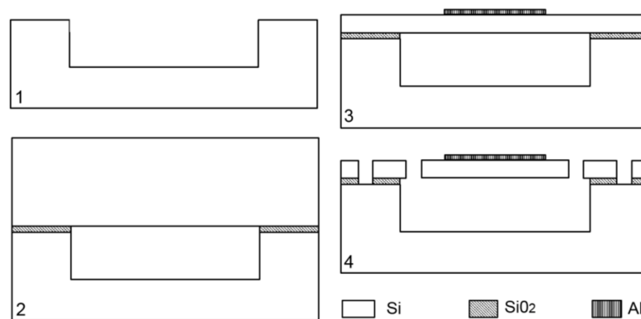

Fig. 3. Process flow for the fabrication of the resonant mirror. (1) A cavity is etched in the substrate wafer; (2) The wafer is oxidized and a SOI structure is formed by anodic bonding; (3) The wafer is thinned down to the desired thickness, the Aluminum reflective layer is evaporated and etched on the surface; (4) Suspended structures are finally released by DRIE etching.

These challenges are shared in the design and construction of the LM that requires a more complicated process due to its fully rotational design. The comb fingers of the rotor and the stator do not lay in the same plane, as can be observed in Fig. 4(a), in order to ensure a linear driving of the mirror: the higher the applied voltage, the stronger the electrostatic force that pulls the rotor fingers towards the stators.

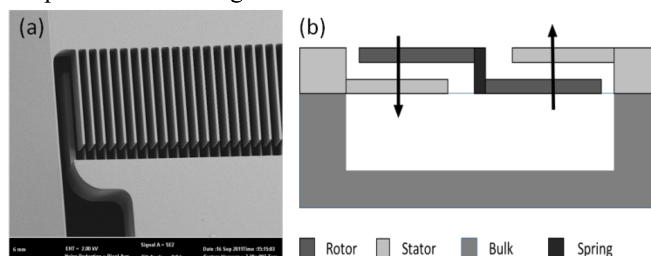

Fig. 4. (a) SEM image of the comb finger region of the linear device. (b) Schematic cross section of the fully rotational configuration.

The fully rotational design requires comb fingers in two separate planes: stator and rotor have fingers on both planes so that the resulting force induces only torsional movements around the spring longitudinal axis [23]. This alternating comb finger structure is repeated specularly four times over the length of the rotor, so that the resulting electrostatic forces are perfectly balanced and ensure pulling in both directions. A schematic view of the cross section of the LM in the selected fully rotational configuration is reported in Fig. 4(b).

In this configuration of the LM neither the stator nor the rotor are a planar structure. The fabrication process requires micromachining of two separate wafers that are then bonded together. The schematic drawings in Fig. 5 illustrate the main fabrication steps for the linear mirror. A bulk Si wafer (or Cap wafer) is employed for the substrate with the cavities (Steps 1-3) whereas an SOI wafer (or MEMS wafer) is used to fabricate rotor, stator and comb finger structure (Steps 4-8). The native SOI wafer is processed from the front side to create the lower part of the three-dimensional stator and rotor structures whereas the cavity for rotor tilting is etched on the cap wafer. A sacrificial TEOS (tetraethylorthosilicate) oxide (SiO_2) layer

Copyright (c) 2014 IEEE. Personal use is permitted. For any other purposes, permission must be obtained from the IEEE by emailing pubs-permissions@ieee.org.

This is the author's version of an article that has been published in this journal. Changes were made to this version by the publisher prior to publication.
The final version of record is available at http://dx.doi.org/10.1109/JSTQE.2014.2369499

is grown on top of the SOI wafer (Step 5); an epitaxial Polysilicon layer is then grown (Step 6) and etched to form the bottom comb finger structures of rotor and stators (Step 7). The Cap wafer is then bonded to the SOI wafer through thermo-compression fusion of metal layers (Step 9). The resulting stack has the backside of the SOI wafer on the top. The top Si layer is then thinned to the desired thickness by means of CMP (Step 10); the top parts of stators and rotor are realized on the remaining crystalline silicon layer by RIE and are released by HF (Hydrofluoric acid) etching of the sacrificial TEOS layer (Steps 11-13). The metallization of the mirror and contact pads, as well as the electrical isolation of the stator and rotor, are completed as for the RM.

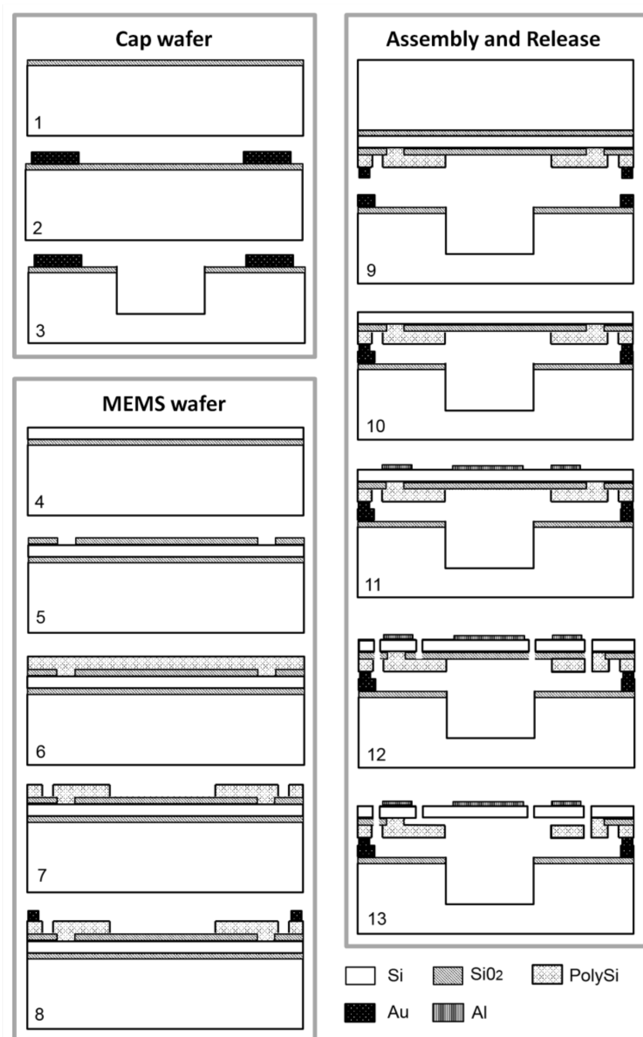

Fig. 5. Process flow for the fabrication of the linear mirror. Cap wafer: (1) TEOS layer grown on the surface; (2) Au structures patterned to form the adhesion layer; (3) DRIE etched cavity. MEMS wafer: (4) starting SOI wafer; (5) TEOS deposition; (6) openings on the TEOS layer as seeds for the growth of the PolySi epitaxial layer; (7) PolySi patterned to form the bottom comb finger structures of rotor and stator; (8) Au layer patterned to form the adhesion structures for wafer bonding. Assembling: (9) Cap and MEMS wafer bonded together via thermo-compression fusion of Au, (10) MEMS wafer is thinned down via CMP; (11) Al layer patterned to form the reflective mirror and the contact pads; (12) deep etching step for releasing the bottom structures; (13) HF etching of the TEOS layer for releasing the upper structures.

Clearly, the LM structure is more complicated than the resonant one. It also results in a larger device since the linear actuation requires more fingers to generate enough torque to tilt the rotor at the desired angle with voltage amplitude lower than 250 V.

As mentioned before, the linear scanning mirror is used to stack the lines projected from the resonant mirror and thus to obtain the two-dimensional image. The actuation mechanism has to quickly bring the mirror back to the correct position before projecting a new image (blanking step). A triangular wave with linear profile, characterized by rise and fall time of different duration (i.e, a sawtooth-like waveform) is applied for LM actuation. In particular, the linear profile with lower slope takes 90 % of the waveform period and the fall time is much shorter, so that the mirror can be quickly brought back to its initial position. Different driving signals for each stator are required. Since they must be always positive, it is necessary to superpose the triangular waveform to an offset between 20 V and 40 V between rotor and stator. These offset voltages, required to pre-charge the structure capacitance, were determined experimentally. Out-of-phase triangular signals on each stator are then required to set the symmetry of the projected line for proper operation of the mirror.

The most efficient way to induce the rotation of the designed resonant micromirror consists in applying to the comb electrodes an always positive square wave with 50% duty cycle at double the frequency of the expected oscillation (solution actually adopted in the picoprojector), since it helps the elastic restoring force in returning the mirror to its rest position every half period [24], [25].

In view of their application, we tested both designs of micromirrors by means of industrial standards for mobile devices. All designs were able to withstand drop and shock test required by the industry to qualify products for use in handheld devices such as mobile phones, laptops and tablets. By design, the springs are able to withstand a stress of more than 3 GP. The linear micromirror has the most critical structure; being linear in nature, its spring is very small with respect to its mass. The linear mirrors reported in this work feature an optimized spring design that makes them able to withstand the required inertial impact of 3000 g in 0.5 ms.

III. Optical Methods for Detection of Micromirror Electro-Mechanical Response

Optical noncontact methods for the characterization of MEMS represent a very important tool for the identification of the experimental behavior of the bare as-fabricated microstructures, since they are not provided with specific transducers and electronic circuits on board for this kind of testing. In particular, spot optical measurements are able to provide valuable information, even in single event [26]-[31], with more compact and simple instrumental configurations, if compared with microscopy imaging techniques.

As previously mentioned, in reflective displays the image projection is obtained by mirror rotations. Thus, mirror testing consists initially in detecting the maximum tilt angle of the reflecting suspended mass. In the case of the linear mirror, the

Copyright (c) 2014 IEEE. Personal use is permitted. For any other purposes, permission must be obtained from the IEEE by emailing pubs-permissions@ieee.org.

This is the author's version of an article that has been published in this journal. Changes were made to this version by the publisher prior to publication.
The final version of record is available at http://dx.doi.org/10.1109/JSTQE.2014.2369499

measurement of the tilt angle must be performed as a function of the applied DC voltage and it corresponds to a characterization of the static behavior of the mirror. In the case of the resonant mirror, the tilt angle is measured as a function of the frequency, at the maximum amplitude of the driving signal.

Since the mirror can be modeled as a suspended mass-spring-damping microsystem, electrostatic driving could induce unwanted displacements, due to vibration modes with out-of-plane and in-plane components, that might produce image distortions [32]. Therefore, an experimental investigation of the dynamic behavior of both the resonant and linear mirrors is required not only with regard to the rotational mode but also to other spurious higher modes [33].

In this work, the performances of the fabricated mirrors, in terms of maximum tilt angle that can be obtained as a result of the rotation around the main axis, are demonstrated using the simple instrumental configuration shown in Fig. 6. It detects the deflection angle variations of a laser beam impinging on the mirror with a 45° incidence angle with respect to the substrate plane, when the mirror is actuated.

The optical setup incorporates a single-transverse mode laser diode, emitting optical power P = 4.5 mW at λ = 635 nm. The collimated laser beam is shone onto the micromirror and reflected toward a semi-transparent target. The detection system for recovering the position of the light spot utilizes a CMOS Logitech camera with 320 x 240 pixels as image sensors. With this set-up, tilt angle measurements can be performed as a function of the applied DC voltage (only on linear mirrors) and as a function of the frequency in a very narrow band centered at the resonance frequency of the rotational fundamental mode. When the mirror rotates, the position of the reflected spot on the detector is changed.

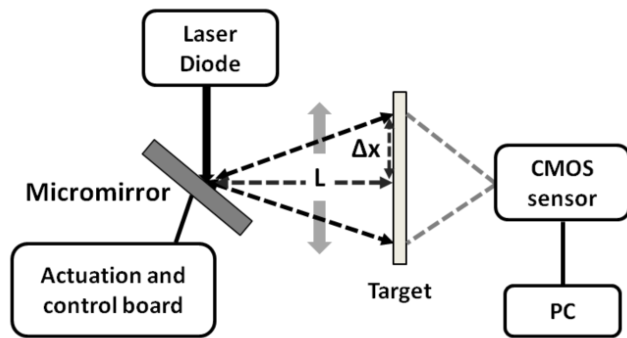

Fig. 6. Instrumental configuration for scanning angle measurements. L is the mirror-target distance and Δx is the half segment length on the target.

By measuring with the CMOS sensor the maximum spot displacement on the target, the mirror tilt angle α_t, with respect to the planar, quiescent position, can be easily calculated, using the well-known relation:

$$\alpha_t = \pm \frac{1}{2} \arctan\left(\frac{\Delta x}{L}\right) \tag{1}$$

and the maximum scanning angle α_s is then given by:

$$\alpha_s = 2 \arctan\left(\frac{\Delta x}{L}\right) \tag{2}$$

where L is the mirror-target distance and Δx is the half segment length, indicated in Fig. 6. Resolution is basically limited by the camera pixel size and depends on L.

In addition to the scanning angle, the dynamic behavior of the micromirrors needs to be investigated, in order to determine the resonance frequencies of higher order vibrating modes. Semiconductor laser feedback (or self-mixing) interferometry performs high-resolution noncontact detection of target displacements and is particularly well suited for micromachined device characterizations. Self-mixing interferometry relies on the interaction between the optical field back reflected or diffused by the remote vibrating target and the laser intra-cavity field. Optical feedback inside the semiconductor laser cavity induces amplitude and frequency modulation of the emitted field, directly related to the propagation phase delay cumulated along the external cavity path [31], [34], [35].

The optical and instrumental configuration for self-mixing interferometry is illustrated in Fig. 7. It incorporates a commercially available, single-mode semiconductor laser (Hitachi HL7851G) emitting at λ = 785 nm and driven above threshold by a constant pumping current $I_p \approx 45$ mA. The use of diode lasers emitting visible light was discarded due to lower efficiency in the generation of the interferometric signal and worse reliability. The laser beam is focused on the micromirrror mounted on a xyz precision translation stage. The monitor photodiode inside the laser package generates a current proportional to the interferometric signal that is converted to a voltage signal by a custom-designed trans-impedance amplifier. The voltage signal can then be viewed with a spectrum analyzer in the frequency domain.

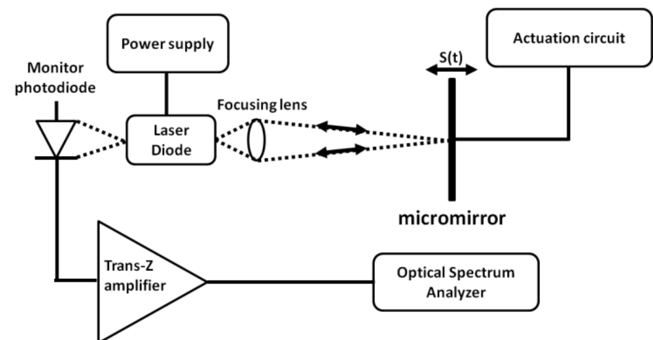

Fig. 7. Optical and instrumental configuration for self-mixing interferometry.

As already reported [31], [34], [35], for very low feedback levels, the photogenerated current can be approximated with the following expression:

$$I(t) \propto I_o \cos\left(2ks_o + 2ks(t)\right) \tag{3}$$

Copyright (c) 2014 IEEE. Personal use is permitted. For any other purposes, permission must be obtained from the IEEE by emailing pubs-permissions@ieee.org.

This is the author's version of an article that has been published in this journal. Changes were made to this version by the publisher prior to publication.
The final version of record is available at http://dx.doi.org/10.1109/JSTQE.2014.2369499

where I_o is the DC component of the interferometric signal, k=2π/λ is the wavenumber, s_o is the laser-target distance and $s(t)$ is the displacement component of the target along the direction of the laser beam. By working in quadrature, we get:

$$I(t) \propto I_o \sin(2ks(t)) \quad (4)$$

and thus, for $s(t) << \lambda/2$, the photodetected current is proportional to the target displacement.

The self-mixing interferometer detects displacement components of the reflecting/diffusing target along the direction of the laser beam. Hence, rotational and out-of-plane oscillating modes can be easily detected when the laser beam direction is perpendicular to the substrate of the MEMS device: in this way, both kinds of vibrations exhibit displacement components along the direction sensed by the interferometer. Discrimination between the rotational and out-of-plane mode can be readily achieved by performing spatially resolved measurements on the rotational axis and on the lateral borders of the mirror. On the other hand, detection of the in-plane mode requires the use of grazing incidence of the laser beam with respect to the substrate of the device, on the mirror edge, so that in-plane displacement of the suspended mass develops a component along the direction of the read-out laser beam. Due to the grazing incidence, back scattering generates optical feedback into the laser cavity. In this case, the superior detection capabilities of self-mixing interferometry on diffusing targets, with respect to classical external interferometers, play a key role for successful measurements.

IV. Characterization of the Resonant Micromirror for Horizontal Image Scanning

Initially, by using the setup reported in Fig. 6 and applying the driving signal to both side stators of the RM, while grounding the rotor, we performed frequency sweeps to determine the scanning angle as a function of the frequency. A 2-Hz frequency step variation was selected in order to properly identify the resonance frequency and the angle. As a consequence of the high angular velocity of the resonant mirror, the CMOS camera visualized the spot displacement on the target due to mirror rotation as a segment; its length is related to the tilt angle of the mirror. The tilt angle as a function of the frequency, measured on two fabricated samples of the resonant micromirror, is displayed in Fig. 8.

In this case, with an amplitude of the driving square-wave of 190 V, the resonance frequency is observed at $f_{rot} \approx 25.4$ kHz where a single-side tilt angle $\alpha_t = 12°$ is obtained. This result ensures the overall horizontal scanning angle $\alpha_s = 48°$ that is required by the design specifications. Given the resonance curves obtained for full displacement, we estimate a 15 Hz tolerance with respect to the actual resonance frequency. This value requires a driving signal of roughly 25.4 kHz and a resolution of 5 Hz at 250 V, which is achievable by HCMOS technology.

For investigating the electro-mechanical frequency response and identifying higher order vibration modes, the mirror was actuated with electrical white noise (on the band of interest) applied between the rotor and stators and we analyzed the self-mixing interferometric signal in the frequency domain. Initially, the laser beam was focused on the mirror at normal incidence with respect to the substrate. To distinguish the resonance frequencies of the rotational and of the out-of-plane mode, spatially resolved measurements were performed by pointing the laser beam in two different positions of the suspended reflecting mass, that is on the rotational axis and on the lateral border. Typical results of these investigations are reported in Fig. 9, where the spectral density of the photodetected interferometric signal is displayed as a function of the frequency in the range 21-33 kHz.

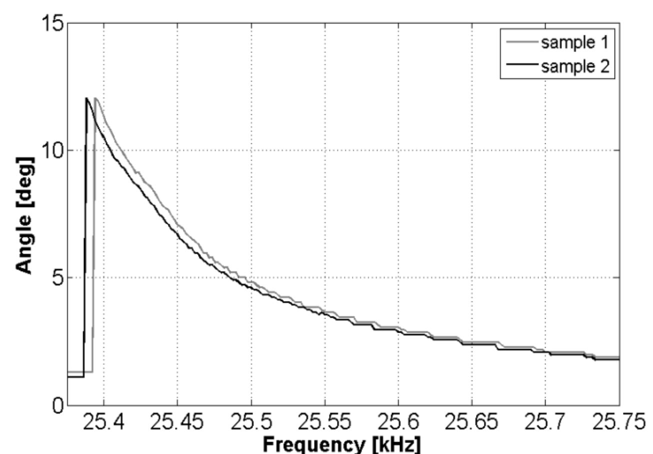

Fig. 8. Tilt angle of the resonant micromirror as a function of the frequency.

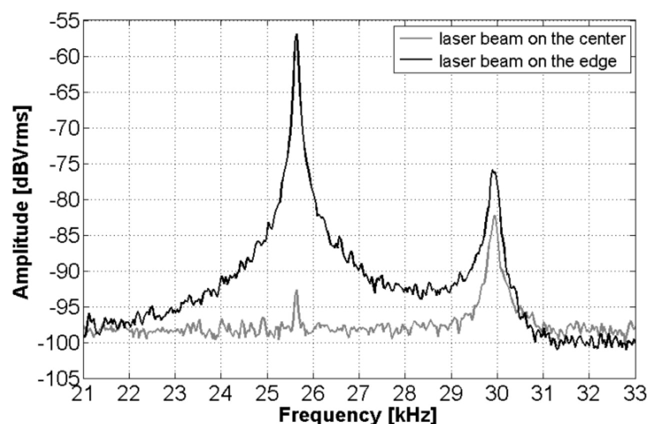

Fig. 9. Frequency response of the resonant model obtained by actuating the device with electrical white noise superposed to a DC voltage V_{DC} = 70 V, and by shining the laser beam perpendicularly with respect to the substrate and in two different positions (on the right side and at the center of the mirror).

As previously demonstrated [36], the photodetected signal is proportional to target displacement, as long as it is much smaller than $\lambda/2$. By directing the laser on the lateral border of the suspended mass, the displacement is due to both the rotational mode at $f_{rot} \approx 25.7$ kHz and the out-of-plane mode at $f_{out\text{-}of\text{-}plane} \approx 29.9$ kHz; the frequency response thus shows two well-defined resonance peaks at frequencies that are in agreement with the values predicted by numerical simulations

Copyright (c) 2014 IEEE. Personal use is permitted. For any other purposes, permission must be obtained from the IEEE by emailing pubs-permissions@ieee.org.

This is the author's version of an article that has been published in this journal. Changes were made to this version by the publisher prior to publication.
The final version of record is available at http://dx.doi.org/10.1109/JSTQE.2014.2369499

with FEM, namely $f_{rot} \approx 25.4$ kHz and $f_{out\text{-}of\text{-}plane} \approx 30.1$ kHz. In the frequency response obtained by hitting the center of the mirror, on the other hand, the main contribution comes from the out-of-plane mode. In practical cases, complete rotational mode suppression is never achieved due to both alignment limitations and finite beam size in the lens focal plane. Indeed, the self-mixing interferometer allows measurements with sufficient spatial resolution to be carried out in order to distinguish the vibration modes. Similar measurements were performed to identify the effect of the applied DC voltage on the resonance curve of the rotational mode and the results are shown in Fig. 10 for V_{DC} = 50, 60, 70 V. The resonance frequency increased by augmenting the applied DC voltage V_{DC}, probably due to a spring hardening effect. As expected with comb finger structures, the actuation efficiency improved with higher values of V_{DC}. Note that the self-mixing interferometer is suitable to detect the small signal response of the device, reported in Fig. 9 and 10, whereas in Fig. 8 the large signal non-linear response is depicted; the non linearity is related to fluid-dynamic effects occurring at atmospheric pressure [22]. In this case, commonly used design criteria are not suitable to predict the dynamic fluid-mechanical damping due to air friction in case of large displacements. A three-dimensional computational fluid dynamics (CFD) model of the air flow around the moving parts of the mirror was developed, coping with dynamic meshing procedures to properly account for the large displacement setting required by the motion of the compliant structures [22].

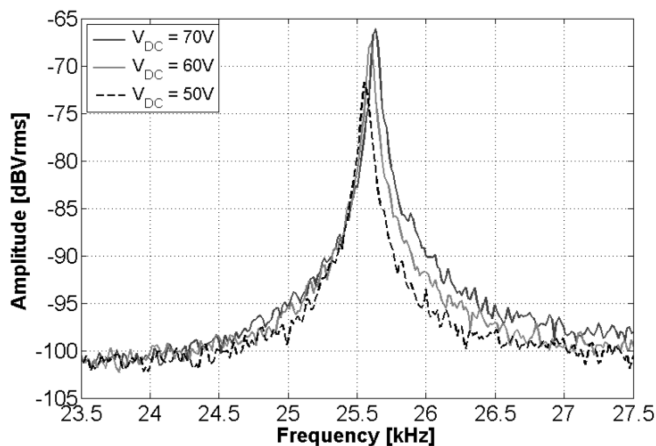

Fig. 10. Effect of the applied DC voltage (V_{DC} = 50, 60, 70 V) on the resonance curve of the rotational mode of the resonant mirror.

For identifying the spectral response of the in-plane mode, laser beam grazing incidence and different actuation scheme were exploited. In particular, the device was driven by applying electrical white noise superposed to the DC voltage V_{DC} = 70 V to a stator and by grounding the rotor and the other stator. With this setup, the spectral response shown in Fig. 11 was typically obtained in the frequency range 24-44 kHz. The resonance curves of the in-plane mode (at higher frequencies, $f_{in\text{-}plane} \approx 39.5$ kHz) as well as of the rotational mode can be distinguished. The FEM predicted value $f_{in\text{-}plane} \approx$ 40 kHz is in agreement with the experimental result.

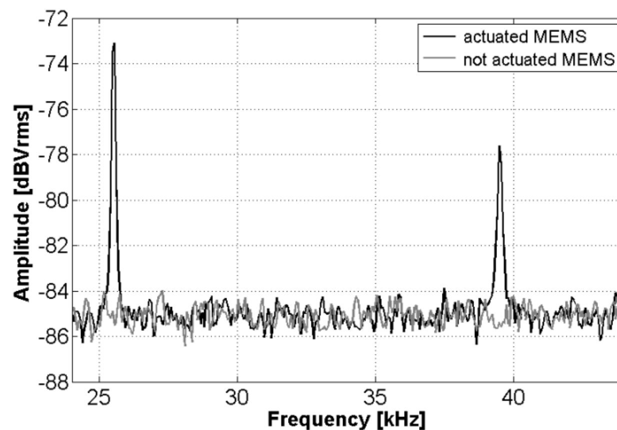

Fig. 11. Frequency response of the resonant mirror obtained with grazing incidence of the laser beam. The resonance curves of the in-plane mode as well as of the rotational mode (at lower frequency) can be distinguished.

V. Characterization of the Linear Micromirror for Vertical Image Scanning

The micromirror for vertical scanning must be driven by a waveform with a frequency in the range of 50-60 Hz, which corresponds to the image frame rate. The linear scanning mirror is used to stack the lines projected from the resonant mirror and thus to obtain the two-dimensional image. It is important to point out that the actuation mechanism has to quickly bring the mirror back to the correct position before projecting a new image (blanking step).

The instrumental configuration reported in Fig. 6 was used to characterize the static behavior of the linear micromirror. To carry out these measurements, only one stator (leaving the other floating) was fed with a constant voltage for tilting the mirror always on the same side and the rotor was grounded. By driving a stator with a DC voltage, the constant electrostatic force generated between the rotor and the stator maintained the mirror tilted at an angle for which the electrostatic and elastic forces were balanced. The spot projected by the mirror on the target during the measurement was captured and, by processing the image data, the value of the tilt angle was obtained. To verify the correct operation of the mirror we tested both stators to demonstrate the structure symmetry. Fig. 12 shows typical results of static measurements demonstrating that the required single-side tilt angle $\alpha_t = 9°$ is obtained at V = 200 V. This result indicates that a vertical scanning angle $\alpha_s = 36°$ can be attained. The dynamic behavior of linear micromirrors was characterized with the self-mixing interferometer shown in Fig. 7. It should be underlined that by driving the linear mirror at the resonance frequency of the rotational mode, the actuation efficiency was greatly increased and wide tilt angles were reached even at low voltages due to the low spring constant.

For dynamic testing, the driving voltage (electrical white noise superimposed to a DC offset voltage) was applied to the rotor, after grounding the stators. As for resonant mirrors, also for linear mirrors spatially resolved measurements were carried out with the laser beam perpendicular to the mirror substrate in two different positions (on the rotational axis and close to the mirror lateral border) in order to distinguish the

Copyright (c) 2014 IEEE. Personal use is permitted. For any other purposes, permission must be obtained from the IEEE by emailing pubs-permissions@ieee.org.

This is the author's version of an article that has been published in this journal. Changes were made to this version by the publisher prior to publication.
The final version of record is available at http://dx.doi.org/10.1109/JSTQE.2014.2369499

rotational mode from the out-of-plane mode. Typical results of these measurements are reported in Fig. 13. Experimental resonance frequencies are $f_{rot} \approx 700$ Hz and $f_{out\text{-}of\text{-}plane} \approx 2.65$ kHz for the rotational and out-of-plane mode, respectively, in agreement with the values obtained with FEM numerical simulations ($f_{rot} \approx 0.71$ kHz and $f_{out\text{-}of\text{-}plane} \approx 2.76$ kHz).

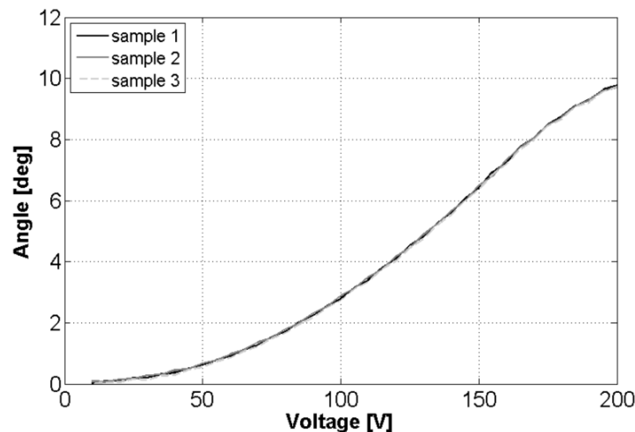

Fig. 12. Mirror tilt angle as a function of the applied DC voltage.

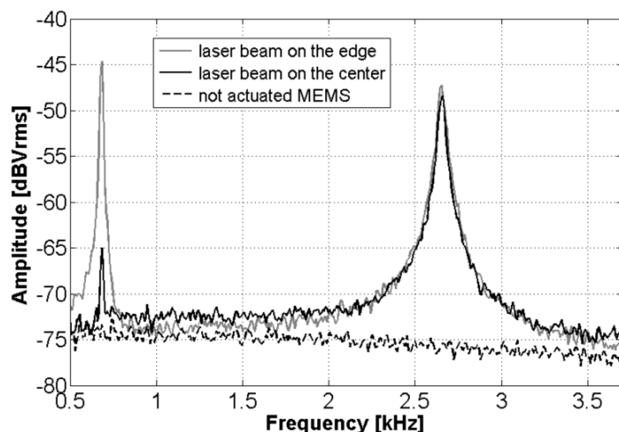

Fig. 13. Frequency response of the linear model obtained by actuating the device with electrical white noise superposed to a DC voltage, measured with the self-mixing interferometer by shining the laser beam perpendicularly with respect to the substrate in two different mirror positions (lateral border and center).

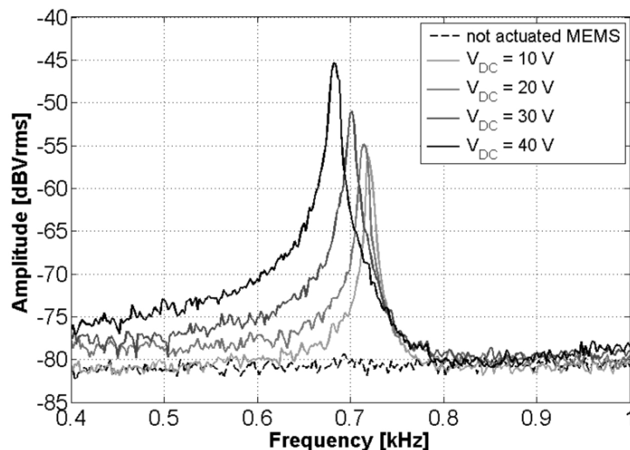

Fig. 14. Effect of the applied DC voltage (V_{DC} = 10, 20, 30, 40 V) on the resonance curve of the rotational mode of the linear mirror.

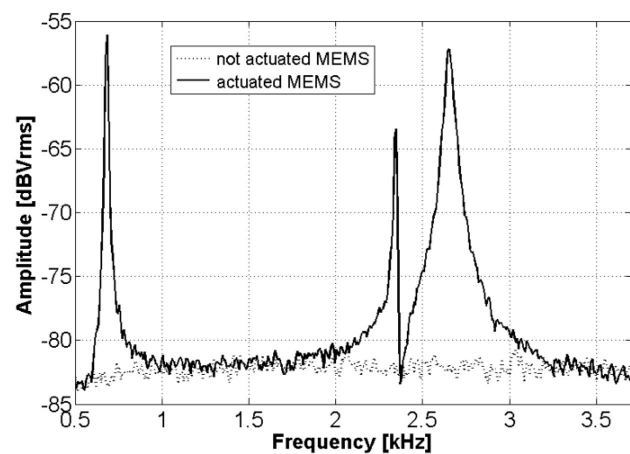

Fig. 15. Frequency response of the linear mirror by actuating the device with electrical white noise superposed to a DC voltage, detected by using the self-mixing interferometer in the grazing incidence configuration.

The effect of the DC voltage on the resonance frequency is reported in Fig. 14. A decrease in the rotational resonance frequency is observed by increasing the DC voltage. The physical layout of the device can be accounted for this particular property, since a higher DC component results in a spring softening effect. On the other hand, augmenting the DC voltage induces an increase of actuation efficiency.

The self-mixing interferometer operating with grazing incidence can identify the resonance frequency of the in-plane translating mode. A typical frequency response measured in this configuration is reported in Fig. 15. By comparing this response to the previously detected resonance frequencies of the rotational and out-of-plane modes, the experimental resonance frequency $f_{in\text{-}plane} \approx 2.35$ kHz confirms the FEM value $f_{in\text{-}plane} \approx 2.32$ kHz.

CONCLUSION

Semiconductor laser feedback interferometry is a powerful optical technique for characterizing the dynamic behavior of rotational micromirrors, with an easy to use and very compact setup. Spot optical measurements based on self-mixing interferometry allowed the detection of the resonance frequencies of the different mechanical vibration modes with sub-micrometric spatial resolution set by the coherent technique. The spectral resolution of the order of 1 Hz was mainly limited by the frequency stability of the driving circuit and by the electrical spectrum analyzer. The experimental values of the resonance frequency of the fundamental rotational mode as well as of the first in-plane and out-of-plane translation modes were found in agreement with the values obtained with FEM. The dynamic behavior of the micromirrors is susceptible to many external factors such as process variations, temperature and pressure. Although these deviations were taken into account in the design phase, the driving circuit of the final picoprojector is designed to track the main resonance frequency of the RM during operation. A capacitive feedback signal acquired at the comb fingers (which is proportional to the actual rotor position) allows the driving circuit to adjust the frequency and amplitude of the

Copyright (c) 2014 IEEE. Personal use is permitted. For any other purposes, permission must be obtained from the IEEE by emailing pubs-permissions@ieee.org.

This is the author's version of an article that has been published in this journal. Changes were made to this version by the publisher prior to publication.
The final version of record is available at http://dx.doi.org/10.1109/JSTQE.2014.2369499

driving signal, to track the steep resonance curve in real time and assure proper operation, despite the presence of uncontrolled external factors.

Measurements of the maximum scanning angle were performed by simple reflectivity measurements employing a laser diode emitting in the visible region. Angle resolution in these measurements was about 3 mrad, only limited by the employed CMOS camera resolution (320 x 240 pixels).

In conclusion, we have demonstrated experimentally that the single-axis rotational micromirrors designed and fabricated by STM are, in terms of scanning angle and frequency response, suitable for high-resolution projectors. For both mirrors, the required driving voltage and the overall size are compatible for proper integration in portable devices.

References

[1] B. Vigna, "More than Moore: micro-machined products enable new applications and open new markets," in *IEEE International Electron Devices Meeting. IEDM Technical Digest* 2005, p. 8, 2005.

[2] B. Vigna, "MEMS Epiphany," in *IEEE 22nd International Conference on Microelectromechanical Systems. MEMS 2009*, pp. 1–6, 2009.

[3] G. Katal, N. Tyagi, and A. Joshi, "Digital Light Processing and its Future Applications," *Int. J. Sci. Res. Publ.*, vol. 3, no. 4, pp. 1–8, 2013.

[4] I. R. S. Chip, "Emerging MEMS: Leading suppliers," *MEMS' trends*, vol. 1, no. 12, pp. 8–11, 2012.

[5] P. F. van Kessel, L. J. Hornbeck, R. E. Meier, and M. R. Douglass, "A MEMS-Based Projection Display," *Proc. IEEE*, vol. 86, no. 8, pp. 1687–1704, 1998.

[6] L. J. Hornbeck, "Digital Light Processing for High-Brightness, High-Resolution Applications," in *Projection Displays III*, *Proc. SPIE,* vol. *3013,* p. 27, 1997.

[7] S. Naik, "Digital Light Processing," *Digit Mag.*, vol. 5, no. 5, pp. 32–34, 2005.

[8] R. J. Gove, V. Markandey, S. Marshall, D. Doherty, G. Sextro, and M. Du Val, "High definition display system based on digital micromirror devices," *Proceedings of the International Workshop on HDTV '94, International Institut for Communication, Turin, Italy*, 1994.

[9] G. Sextro, T. Ballew, and J. Iwai, "High-definition projection system using DMD display technology," *SID International Symposium Digest of Technical Papers. SOCIETY FOR INFORMATION DISPLAY*, vol. 26, pp. 70–73, 1995.

[10] J. M. Younse, "Projection display systems based on the Digital Micromirror Device (DMD)," in *Microelectronic Structures and Microelectromechanical Devices for Optical Processing and Multimedia Applications*, *Proc. SPIE,* vol. *2641,* pp. 64–75, 1995.

[11] K. E. Petersen, "Silicon Torsional Scanning Mirror," *IBM J. Res. Dev.*, vol. 24, no. 5, p. 631, 1980.

[12] H. Schenk, P. Durr, D. Kunze, H. Lakner, and H. Kuck, "An electrostatically excited 2D-micro-scanning-mirror with an in-plane configuration of the driving electrodes," in *The 13th Annual International Conference on Microelectromechanical Systems. MEMS 2000*, pp. 473–478, 2000.

[13] J. Fritz, S. Pinter, C. Friese, T. Pirk, and H. Seidel, "Microscanner using self-aligned vertical comb drives in a switched electrode configuration for large static rotation," in *IEEE/LEOS International Conference on Optical MEMS and Nanophotonics,* pp. 37–38, 2009.

[14] M. Freeman, M. Champion, and S. Madhavan, "Scanned Laser Pico-Projectors: Seeing the Big Picture (with a Small Device)," *Opt. Photonics News*, vol. 20, no. 5, pp. 28–34, 2009.

[15] W. O. Davis, R. Sprague, and J. Miller, "MEMS-based pico projector display," in *IEEE/LEOS International Conference on Optical MEMS and Nanophotonics,* pp. 31–32, 2008.

[16] "STMicroelectronics and bTendo to Develop the World's Smallest Focus-Free Embedded Pico-Projector for Next-Generation Smart Phones." http://www.st.com/web/en/press/en/t3130.

[17] U. Hofmann, J. Janes, and H. Quenzer, "High-Q MEMS Resonators for Laser Beam Scanning Displays," *Micromachines*, vol. 3, pp. 509–528, 2012.

[18] H. Urey, D. W. Wine, and T. D. Osborn, "Optical performance requirements for MEMS-scanner-based microdisplays," in *MOEMS and Miniaturized Systems, Proc. SPIE,* vol. *4178,* pp. 176–185, 2000.

[19] A. D. Yalcinkaya, H. Urey, D. Brown, T. Montague, and R. Sprague, "Two-Axis Electromagnetic Microscanner for High Resolution Displays," *J. Microelectromechanical Syst.*, vol. 15, no. 4, pp. 786–794, 2006.

[20] H. Urey, "Torsional MEMS scanner design for high-resolution display systems," in *Optical Scanning II*, *Proc. SPIE, vol. 4773,* pp. 27–37, 2002.

[21] S. T. S. Holmström, U. Baran, H. Urey, and S. Member, "MEMS Laser Scanners: A Review," *J. Microelectromechanical Syst.*, vol. 23, no. 2, pp. 259–275, 2014.

[22] R. Mirzazadeh, S. Mariani, A. Ghisi, and M. De Fazio, "Fluid damping in compliant, comb-actuated torsional micromirrors," in *15th International Conference on Thermal, Mechanical and Multi-Physics Simulation and Experiments in Microelectronics and Microsystems*, pp. 1–7, 2014.

[23] Y. Mizoguchi and M. Esashf, "Design and Fabrication of a Pure-Rotation Microscanner with Self-Aligned Electrostatic Vertical Combdrives in Double SOI wafer," in *The 13th Conference on Solid-State Sensors, Actuators and Microsystems. TRANSDUCERS '05*, *Digest of Technical Papers,* pp. 65–68, 2005.

[24] W. Schock, J. Mehner, J. Fritz, J. Muchow, C. Friese, and S. Pinter, "FEM based modeling and optimization of a 2D micro mirror," in *Proc. of 12th International Conference on Thermal, Mechanical and Multi-Physics Simulation and Experiments in Microelectronics and Microsystems*, pp. 1–6, 2011.

[25] C. Lee, "Design and fabrication of epitaxial silicon micromirror devices," *Sensors and Actuators A*, vol. 115, no. 2, pp. 581–590, 2004.

[26] J. S. Burdess, A. J. Harris, D. Wood, R. J. Pitcher, and D. Glennie, "A System for the Dynamic Characterization of Microstructures," *J. Microelectromechanical Syst.*, vol. 6, no. 4, pp. 322–328, 1997.

[27] F. M. Dickey, S. C. Holswade, L. A. Hornak, and K. S. Brown, "Optical methods for micromachine monitoring and feedback," *Sensors and Actuators A*, vol. 78, no. 2–3, pp. 220–235, 1999.

[28] H. Kim, J. Kim, and H. Shin, "A laser-based 2-dimesional angular deflection measurement system for tilting microplates," *Sensors and Actuators A*, vol. 86, no. 1–2, pp. 141–147, 2000.

[29] V. Annovazzi-Lodi, S. Merlo, M. Norgia, G. Spinola, B. Vigna, and S. Zerbini, "Optical Detection of the Coriolis Force on a Silicon Micromachined Gyroscope," *J. Microelectromechanical Syst.*, vol. 12, no. 5, pp. 540–549, 2003.

[30] V. Annovazzi-Lodi, S. Merlo, and M. Norgia, "Characterization of silicon microstructures by feedback interferometry," *J. Opt. A: Pure Appl. Opt.*, vol. 4, no. 6, p. S311, 2002.

[31] V. Annovazzi-Lodi, M. Benedetti, S. Merlo, and M. Norgia, "Spot Optical Measurements on Micromachined Mirrors for Photonic Switching," *IEEE J. Sel. Top. Quantum Electron.*, vol. 10, no. 3, pp. 536–544, 2004.

[32] C. Liu, *Foundations of MEMS*. Upper Saddle River, New Jersey: Prentice Hall, 2005.

[33] H. Urey, C. Kan, and C. Ataman, "Dynamic Modelling of Comb-Driven Microscanners," in *IEEE/LEOS Optical MEMS, Paper I4, 2004*.

[34] S. Merlo, V. Annovazzi-Lodi, M. Benedetti, F. Carli, and M. Norgia, "Tsting of 'Venetian-Blind' Silicon Microstructures with Optical Methods," *J. Microelectromechanical Syst.*, vol. 15, no. 3, pp. 588–596, 2006.

[35] S. Donati, G. Giuliani, and S. Merlo, "Laser Diode Feedback Interferometry for Measurements of Displacements without Ambiguity," *IEEE J. Quantum Electron.*, vol. 31, no. 1, pp. 113–119, 1995.

[36] S. Merlo and S. Donati, "Reconstruction of Displacement Waveforms with a Single-Channel Laser-Diode Feedback Interferometer," *IEEE J. Quantum Electron.*, vol. 33, no. 4, pp. 527–531, 1997.

Gloria Silva was born in Castel San Giovanni (PC), Italy, in 1981. She graduated in Electronic Engineering at the University of Pavia in 2010, with a thesis on the study and realization of a diode-pumped passively mode-locked high repetition rate solid-state laser. She received a Ph.D. degree in Electronic Engineering and Computer Science from the

Copyright (c) 2014 IEEE. Personal use is permitted. For any other purposes, permission must be obtained from the IEEE by emailing pubs-permissions@ieee.org.

This is the author's version of an article that has been published in this journal. Changes were made to this version by the publisher prior to publication.
The final version of record is available at http://dx.doi.org/10.1109/JSTQE.2014.2369499

University of Pavia, Italy, in 2014 with a dissertation entitled "Optical 3D silicon microstructures: advanced characterization methods and applications." Her current research interests include biosensors, photonic crystals, silicon micromachined devices, nanomedicine and gold nanoporous microstructures. She is the co-author of more than 20 publications, including ISI indexed journals and conference proceedings.

Francesca Carpignano (M'2010) was born in Broni (PV), Italy, in 1985. She graduated cum laude in Biomedical Engineering at the University of Pavia in 2010, with a thesis on micro-opto-fluidic devices for photonic crystal biosensors. She received a Ph.D. degree in Bioengineering and Bioinformatics from the University of Pavia, Italy, in 2014 with a dissertation on a new 3D silicon microstructure for simultaneous cell culture and label-free optical transduction. Her current research interests include biosensors, microfluidics, photonic crystals, silicon micromachined devices, lab-on-chip, nanomedicine and cell culture. She is the co-author of more than 40 publications in journals, books and conference proceedings.
Dr. Carpignano is a Student Member of IEEE and of AEIT.

Federica Guerinoni received the B.Sc. and M.Sc. degrees both in Biomedical Engineering from University of Pavia, Italy, in 2006 and 2009, respectively.
After completing her studies, she joined STMicroelectronics, Agrate Brianza, Italy, as a Research Engineer and she played an important role in the development of the characterization setup of MEMS micromirror. Now she works within the STMicroelectronics site of Cornaredo, Mi, Italy, on MEMS microphone characterization.

Sonia Costantini achieved a Master degree in Physics in 1999, with a thesis focused on atomic structure and evolution of Polysilicon triple junctions. In 1999, she joined STMicroelectronics working for the Central Research and Development team. Till 2011 her main activities were focused on Non Volatile Memory (Flash NOR and NAND, Phase Change Memory) and on CMOS.
Since 2011 she is a member of the MEMS technology Research and Development team at STM, working on Optical and Environmental sensors and Actuators.

Marco De Fazio received the Master degree in Nuclear Engineering (solid state physics) from Politecnico di Milano, Italy. In 2001, he worked for STMicroelectronics in lab-on-chip design, fabrication and analog front-end with expertise in sensors' electrical characterization. In 2002, he worked in R&D developing instrumentations for lab-on-chip. Since 2003 till 2005 he was at National Nanotechnology Lab in Lecce attending a joint lab between INFM and ST developing application in the field lab on chip and chemical sensors. Since then he has been working for ST-AST (Advanced System Technologies) in Agrate, Mi, developing microfluidic devices for healthcare applications. He partecipated in several European Research Projects and currently is Adjunct Assistant Professor at the Politecnico di Milano. Since 2008 he has been working on MEMS, photonics and microfluidics, with focus on applications and prototyping of demos, leading the "More than Moore" research lab with the mission of supporting product divisions with longer term research. He is now Scientific Advisor for "More than Moore" research with the aim of exploring new fields for silicon technology applications supporting division in non-conventional longer term research in the field of sensors (MEMS, MOEMS), healthcare and optical systems and, currently, is visiting scientist at MIT with focus on GaN and Graphene.

Sabina Merlo (M'2001-SM'2005) was born in Pavia, Italy, in 1962 and received a degree in Electronic Engineering from the University of Pavia in 1987. She was the recipient of a Rotary Foundation Graduate Scholarship for study at the University of Washington, Seattle (WA), U.S.A. In 1989, she received a M.S.E. degree in Bioengineering from the University of Washington. In 1991, she received a Ph.D. degree in Electronic Engineering from the University of Pavia. In 1993, she became Assistant Professor and, in 2001, she became Associate Professor in the Department of Electronics at the University of Pavia. Her main research interests include optical measurements on silicon micromachined devices (MEMS, MOEMS, photonic crystals), optical interferometry, chaos in lasers, fiber-optic passive components and sensors, and optical biosensors. She holds four patents and is the co-author of more than 100 publications in journals, books and conference proceedings. She is an Associate Editor of the IEEE/ASME Journal of Microelectromechanical Systems.
Dr. Merlo is a member of AEIT, and Senior Member of IEEE-Photonics Society.

Copyright (c) 2014 IEEE. Personal use is permitted. For any other purposes, permission must be obtained from the IEEE by emailing pubs-permissions@ieee.org.